Quark Matter 2005: Experimental Conference Summary

Itzhak Tserruya [a]

[a]Department of Particle Physics, Weizmann Institute of Science, Rehovot 76100, Israel

Highlights of the experimental results presented at the Quark Matter 2005 Conference in Budapest (Hungary) are reviewed and open issues are discussed.

1. Introduction

This was an excellent conference. For the fourth consecutive time since the beginning of RHIC operation in the year 2000, the Quark Matter conference displayed the strong vitality and enormous productivity of the field. A few facts and numbers easily prove this point. Since the last Conference in Oakland 19 months ago, (i) there have been two very successful additional runs at RHIC, run-4 and run-5, basically completing a broad survey of the physics landscape not only in Au+Au collisions at the top RHIC energy of $\sqrt{s_{NN}}$=200 GeV but also at a lower energy, 62 GeV and in a lighter system, Cu+Cu at $\sqrt{s_{NN}}$=200, 62 and 22.5 GeV, and including the crucial reference runs p+p and d+Au at 200 GeV, (ii) I counted 87 papers published in the refereed literature, 30 of them in Phys. Rev. Lett., (iii) monumental White Papers [1] based on the first three years of RHIC operation, were published by the four RHIC experiments reflecting their assessment on the nature of the matter formed at RHIC and a new logo was born, the "perfect fluid". All this and numerous new experimental results from RHIC and SPS formed the core of the 25 and 60 experimental talks given in plenary and parallel sessions, respectively, which I shall try to summarize here.

The last three Quark Matter conferences were naturally dominated by RHIC data, more precisely RHIC data on global event characterization (multiplicity, flow, HBT, fluctuations, kinetic and chemical equilibrium) and the newly discovered high p_T phenomena. This conference was also dominated by RHIC data. But with the advent of results from the high luminosity runs, the emphasis moved to penetrating and rare probes (charm, charmonium, dileptons and photons). High p_T phenomena and jet physics remained a very strong topic. It is also noteworthy that first results were presented from the Cu+Cu run-5 which ended just a few months prior of the conference. The timely release of results is an impressive feature characteristic of all RHIC runs so far. This remarkable achievement would not be possible without the dedication and enthusiasm of many young (and not so young) and brilliant researchers who for several months worked literally around the clock, forgetting week-ends and other obligations, to bring their analyses to the high level required at this conference. I wish to pay tribute to all of them here.

In addition to the RHIC data, we have also seen results from NA60, a second generation experiment at the CERN SPS devoted to the measurement of the dimuon spectrum

from the low-masses up to the J/ψ. With its two main characteristic features, excellent mass resolution and high statistics, NA60 presented superb data from its first run (that unfortunately also seems to be its last one) on In+In at 158 AGeV.

In coming to summarize this conference, it is obviously impossible to do justice to all the new results presented. This summary presents a broad choice, but it is a personal one, and I apologize to all the speakers whose results I could not include in the limited space of this summary.

2. Elliptic Flow

We have seen at this conference many new results on flow mainly from RHIC but also from SPS. Perhaps the most striking result is that open charm, inferred from measurements of inclusive electrons after subtraction of hadron decays, exhibits elliptic flow of comparable magnitude to that of hadrons. This result and the challenge to energy loss models will be discussed in Section 6. Elliptic flow measurements at RHIC have been reported for many new particles, including heavy and rare particles, in particular d and multistrange hadrons, ϕ, Ξ and Ω, (see Fig. 1) [2,3]. So far, *all* hadrons measured at RHIC show elliptic flow. The only notable particle where no results are as yet available is the J/ψ. I shall return to the importance of this missing measurement again in Section 7.

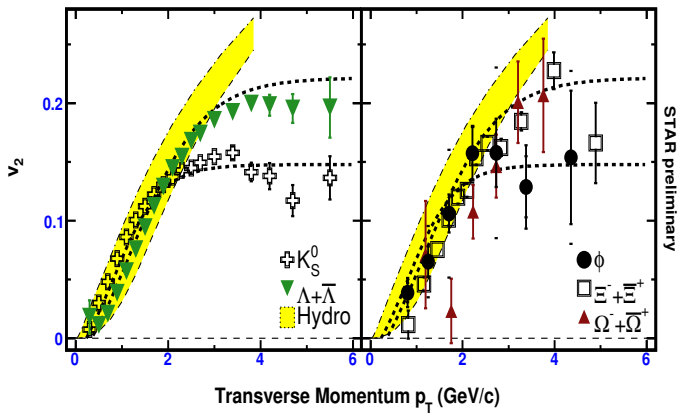

Figure 1. Elliptic flow parameter v_2 for strange (left) and multi-strange (right) hadrons measured by STAR in Au+Au collisions at $\sqrt{s_{NN}}$= 200 GeV. The curves are empirical fits. Hydrodynamic calculations are shown by the shaded areas [4].

All the new RHIC results follow and confirm the pattern already established over the last few years from the wealth of data available on this topic (see the comprehensive review of Lacey at this conference [5]): at low p_T (p_T smaller than $\sim$ 2 GeV/c) v_2 increases monotonically with p_T and the results are well reproduced by hydrodynamic calculations. In the "intermediate" p_T region (p_T = 2-5 GeV/c) the elliptic flow flattens and the hydrodynamic description breaks down as shown e.g. in Fig. 1. The data in this range follow remarkably well the scaling with the number of valence quarks predicted by recombination models [6,7] [1]. This is illustrated in Fig. 2 which shows a comprehensive compilation of elliptic flow measurements with such a scaling. Deviations are seen at low p_T where the hydrodynamic description works best but at intermediate p_T quark scaling works. This

[1]quark scaling is predicted in the limiting case where the combining quarks carry the same fraction of the hadron momentum.

suggests that quarks are the relevant degrees of freedom very early in the collision, when flow takes place. However, it should be stressed that these are constituent quarks.

The measurements of v_2 have been extended to higher p_T values [8,9]. v_2 decreases but retains a non-zero value up to $p_T = 10$ GeV/c, a behavior that is consistent with energy loss models.

The new RHIC flow results contribute to strengthening the case for a strongly interacting quark-gluon plasma, sQGP, characterized by early thermalization of partonic matter made of constituent quarks, behaving like a perfect fluid.

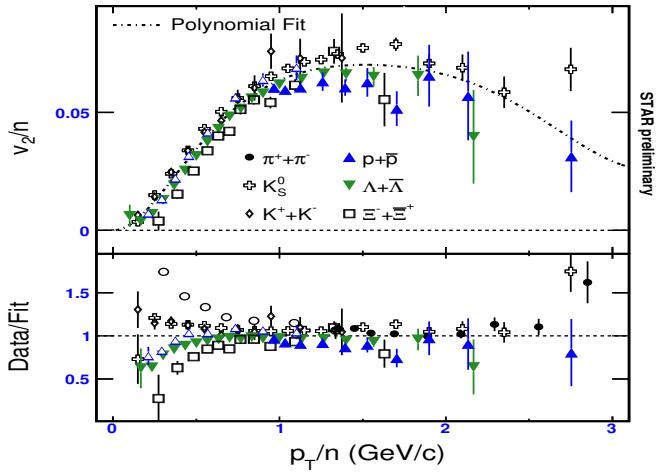

Figure 2. v_2/n vs. p_T/n where n is the number of valence quarks, illustrating the constituent quark scaling of elliptic flow. The bottom panel shows the deviations of the measurements from an empirical fit through all data points [2].

SPS is catching up on flow. Λ v_2 results, from measurements done in the year 2000 at 158 AGeV, were shown by NA49 [10] and CERES [11]. The two are in good agreement with each other. At low p_T, v_2 increases monotonically, as at RHIC energies, but the absolute values are lower at the SPS and hydrodynamic calculations cannot simultaneously reproduce particle spectra and flow. When constrained to reproduce the particle spectra, the hydrodynamic calculations overestimate the amount of flow.

3. Varying the system size: Cu+Cu vs. Au+Au

What new information could be gained by studying different systems at the same energy? This question has come up repeatedly over the years. Proponents have proposed this as an additional knob to turn for the systematic study of relativistic heavy-ion collisions. Clearly the initial geometrical overlap volume in central Cu+Cu collisions has not the same shape as in Au+Au collisions at the selected centrality corresponding to the same number of participants. But if the system quickly expands and reaches thermal equilibrium, this difference could rapidly be erased from the collision memory. Therefore opponents have argued that going to lighter systems would be equivalent to study a heavier one as function of centrality.

The many new results from the recent Cu+Cu run at RHIC provided a clear answer: Cu+Cu is very similar to Au+Au when the two systems are compared for collisions with the same number of participants. A very nice example is shown in Fig. 3 which compares the charged hadron pseudorapidity distributions measured by PHOBOS in Cu+Cu and Au+Au collisions at $\sqrt{s_{NN}}$ =200 GeV [12]. The two distributions are almost identical

when the centrality bins are chosen to correspond to the same number of participants. The same holds true for other centralities and also at $\sqrt{s_{NN}} = 62.4$ GeV [12].

Many other examples supporting this argument were provided by the four RHIC experiments (see [3,12–14]). I shall mention two more: PHOBOS [12] showed that the elliptic flow v_2 relative to the participant eccentricity scales with $N_{\rm part}$ irrespective of the collision system (see also [15]). The J/ψ production also scales with the number of participants and this was demonstrated by the PHENIX results obtained in Au+Au and Cu+Cu collisions (see Section 7) and also at SPS in a comparison of the Pb+Pb and In+In results from NA50 and NA60, respectively.

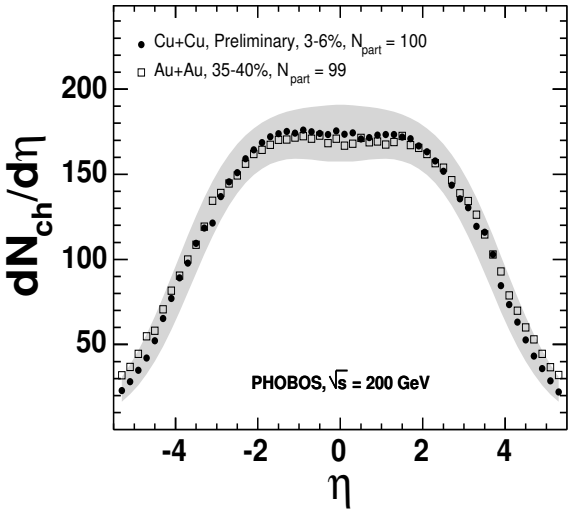

Figure 3. Charged hadron pseudorapidity distribution in $\sqrt{s_{NN}} = 200$ GeV Cu+Cu and Au+Au collisions with similar $N_{\rm part}$ [12].

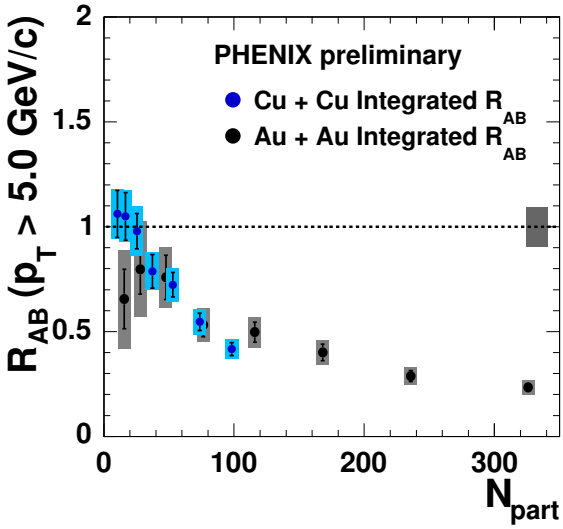

Figure 4. Nuclear modification factor $R_{\rm AA}$ for π^0 vs. $N_{\rm part}$ in central Cu+Cu and Au+Au collisions at $\sqrt{s_{NN}} = 200$ GeV [3].

There is however a real intrinsic benefit in the study of a light system. It adds significant precision to the determination of $N_{\rm part}$ for $N_{\rm part} \leq 100$. This is illustrated in Fig. 4 which compares the nuclear modification factor $R_{\rm AA}$ of π^0 in Cu+Cu and Au+Au collisions vs. $N_{\rm part}$[3]. The same behavior is observed in the two systems for the same $N_{\rm part}$ but the systematic uncertainties are significantly lower in Cu+Cu (see also [12,13]).

4. High p_T hadrons

The suppression of high p_T hadrons in central Au+Au collisions is among the unique and most significant phenomena discovered at RHIC. With the high luminosities of run-4 and run-5 it became possible to extend the p_T reach to much higher values and to perform more detailed and higher precision studies. The new data presented at the conference reinforce the current interpretation in terms of energy loss in a dense and opaque medium but also raise questions and problems about the energy loss mechanisms (see the dedicated reviews on high p_T physics [16,17]) in particular the very intriguing and challenging results on charm suppression which will be discussed in Section 6.

Fig. 5 shows the nuclear modification factor of π^0 measured by PHENIX in central Au+Au collisions at $\sqrt{s_{NN}} = 200$ GeV [18]. The suppression is very strong, with $R_{\rm AA}$

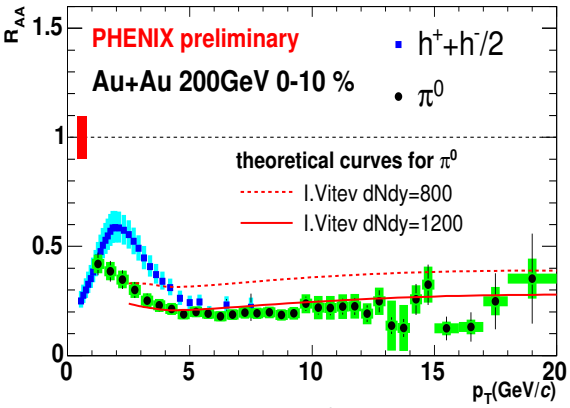

Figure 5. $R_{\rm AA}$ for π^0 and charged hadrons in central Au+Au collisions from PHENIX [18] together with radiative energy loss calculations [19].

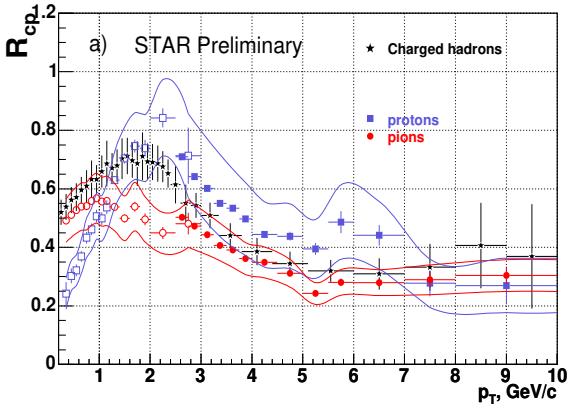

Figure 6. $R_{\rm CP}$, the ratio of N_{binary}-scaled p_T spectra between central (0-5%) and peripheral (60-80%) Au+Au collisions at $\sqrt{s_{NN}}$ = 200 GeV of π, p and charged hadrons [22].

$\sim$0.2, and remains flat up to 20 GeV/c. Very similar results were shown for Cu+Cu [18]. This behavior is well reproduced by partonic radiative energy loss models [19–21]. The figure shows one such calculation implying an average gluon density $dN_g/dy \sim 1200$ [19]. The figure also displays the $R_{\rm AA}$ of charged hadrons. The difference between charged hadrons and π^0's in the "intermediate" p_T region (p_T $\sim$2-5 GeV/c), attributed to the proton contribution and explained by recombination models, disappears at $p_T > 5$ GeV/c in agreement with the same recombination models (not shown) [6,23,24]. Similar results are shown in Fig. 6 which compares the $R_{\rm CP}$ of π and p [22].

NA49 and NA57 presented $R_{\rm CP}$ results at the top SPS energy $\sqrt{s_{NN}}$= 17.3 GeV providing much needed information on the energy dependence of high p_T suppression [25,26]. Results are shown in Fig. 7 for K^0_S and Λ from NA57 compared to similar data from STAR (left panel) and π and p from NA49 (right panel). The same systematic behavior

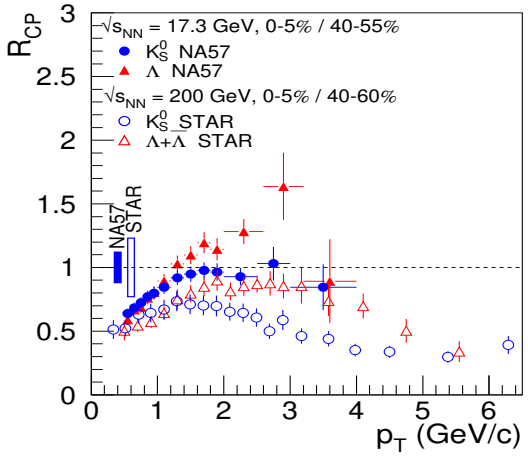

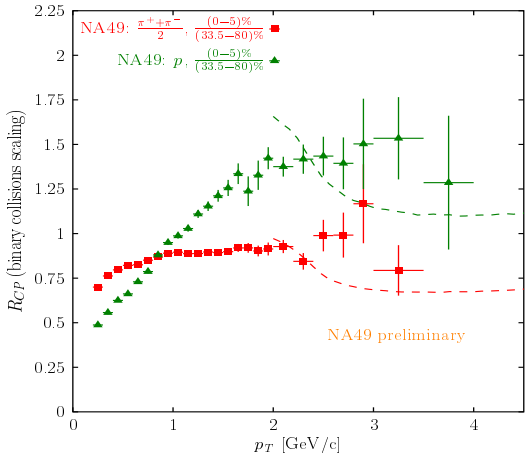

Figure 7. $R_{\rm CP}$ results from SPS. Left panel: results from NA57 for K^0_S and Λ compared to similar data from STAR [26]. Right panel: results from NA49 for p and π [25].

as in RHIC is observed, $R_{\rm CP}$(baryon) > $R_{\rm CP}$(meson) and radiative energy loss models do quite well in reproducing the SPS results. The high p_T suppression is much weaker

than at RHIC but it is strong enough that the expected Cronin enhancement at high p_T is not observed for mesons. The SPS data as well as the preliminary results obtained at the intermediate RHIC energy of $\sqrt{s_{NN}}$= 62.4 GeV [27] are reproduced with an initial gluon density of dN_g/dy that scales as the particle density dN_{ch}/dy [20]. Like with many other observables, there seems to be a smooth energy dependence of the high p_T hadron suppression from SPS to top RHIC energies.

All these results, from RHIC and SPS, appear as a great victory for the partonic energy loss models. However, new results presented at the conference will allow more stringent tests of the models. In particular, results on the dependence of the π^0 suppression on the emission angle with respect to the reaction plane, as function of p_T and centrality [8], will be very valuable in elucidating the interplay of elliptic flow and energy loss as function of p_T and particularly in the intermediate p_T range where the energy loss models fail in reproducing the large values of v_2 [28].

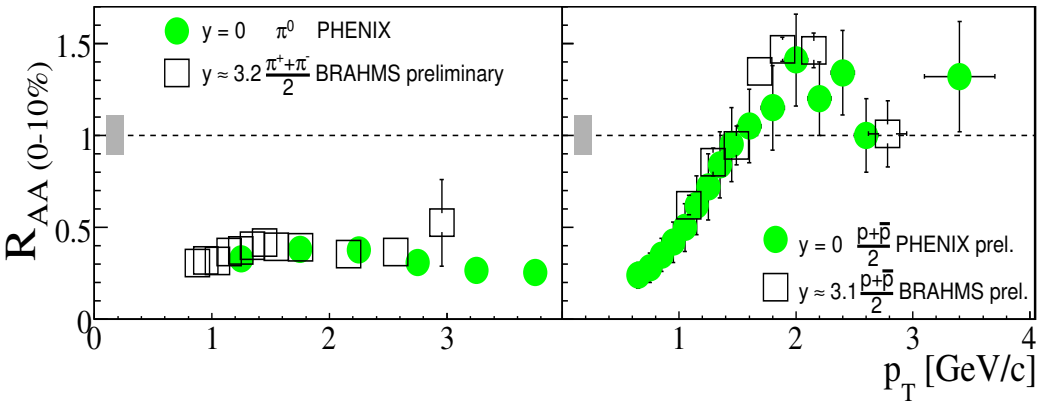

Figure 8. $R_{\rm AA}$ for π (left panel) and p (right panel) measured by BRAHMS at $y = 3.2$ and by PHENIX at $y = 0$ in central Au+Au collisions at $\sqrt{s_{NN}}$= 200 GeV [14].

BRAHMS provided clear evidence that $R_{\rm AA}$ does not depend on rapidity as demonstrated in Fig. 8. The figure shows excellent agreement between the $R_{\rm AA}$ for π and p measured by BRAHMS at $y = 3.2$ and same data measured by PHENIX at $y = 0$ in central Au+Au collisions [14]. This is a surprising result and a challenge for theory. In the jet quenching models, the gluon density is smaller at forward rapidity and consequently one would expect a lower suppression. As a possible explanation one could argue that at forward rapidity, other mechanisms are present, like gluon saturation as manifest in d+Au measurements, that could lead to an additional suppression such that by accident the total suppression looks similar to the one at mid-rapidity [29]. A quantitative analysis incorporating all effects in a comprehensive theoretical approach is needed.

5. Jet correlations

With the availability of large data sets it is now possible to study particle correlations over a large range of p_T values both for the trigger as well as for the associated particles. Each selection of kinematic cuts provides a slice of the jet structure and reveals limited but valuable information. Combining all these selections together should eventually lead to a detailed reconstruction of the jet topology and its interaction with the medium allowing

complete tomography of the matter created at RHIC.

First jet studies at RHIC provided the by now classical result of the away-side jet disappearance in central Au+Au at high p_T values ($p_T^{\rm trig} > 4$ GeV/c and $p_T^{\rm assoc} > 2$ GeV/c) [30]. This dramatic result reflects the limited ability to extract the suppressed away-side jet from the high background in this particular kinematic cut rather than a real disappearance of the jet. If one includes softer associated particles ($0.15 < p_T^{\rm assoc} < 2$ GeV/c while keeping the same trigger $p_T^{\rm trig} > 4$ GeV/c), the correlation strength grows faster than the background and a clear and broad away-side peak appears as shown in recent studies [31]. From these two observations a picture emerges which is fully compatible with parton energy loss in a high-density medium: the hadron trigger preferentially selects a dijet produced near to the surface. The parton heading outwards gives rise to an almost unaffected near-side jet that fires the trigger whereas the recoiling parton looses energy while traversing the medium and its momentum gets redistributed over several particles, suppressing high p_T particles (disappearance of away side peak in [30]) and enhancing low p_T particles (broad away side peak in [31]).

New and additional insights are provided by extending the kinematic cuts to different p_T values. Two prominent examples presented at the conference, of jet correlations at high and intermediate p_T values, are displayed in Figs. 9 [32] and 10 [33], respectively.

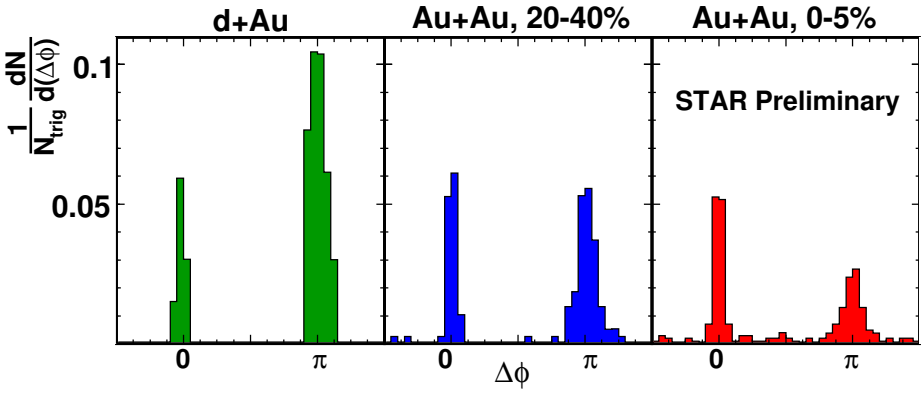

Figure 9. Azimuthal correlations of charged hadrons ($8 < p_T^{\rm trig} < 15$ GeV) with associated particles (6 GeV/c $< p_T^{\rm assoc} < p_T^{\rm trig}$) in d+Au, semi-central (20-40%) and central (0-5%) Au+Au collisions [32].

Fig. 9 shows jet correlations selected with high p_T trigger ($8 < p_T^{\rm trig} < 15$ GeV/c) and high p_T associated particles (6 GeV/c $< p_T^{\rm assoc} < p_T^{\rm trig}$), in minimum bias d+Au, 20-40% Au+Au and 0-5% Au+Au, collisions. Very clear and almost background free back-to-back jets are observed in all three cases and in particular in central Au+Au, in sharp contrast with the away side jet disappearance in central Au+Au at lower p_T values ($p_T^{\rm trig} > 4$ GeV/c and $p_T^{\rm assoc} > 2$ GeV/c) previously discussed. Furthermore, while the away side yields decrease, as expected, from d+Au to central Au+Au, the near side yields are the same for the different systems in contrast with calculations [34]. This new kinematic cut provides new constraints and challenges to theoretical models of jet quenching.

Fig. 10 shows the jet correlation patterns measured by PHENIX with intermediate p_T trigger ($2.5 < p_T^{\rm trig} < 4$ GeV) and intermediate p_T associated particles ($2 < p_T^{\rm assoc} < 3$ GeV/c) [33]. Clear modifications of the away side jet as function of centrality are seen: a broad peak is observed in peripheral collisions that develops a dip at $\Delta\phi = \pi$ with

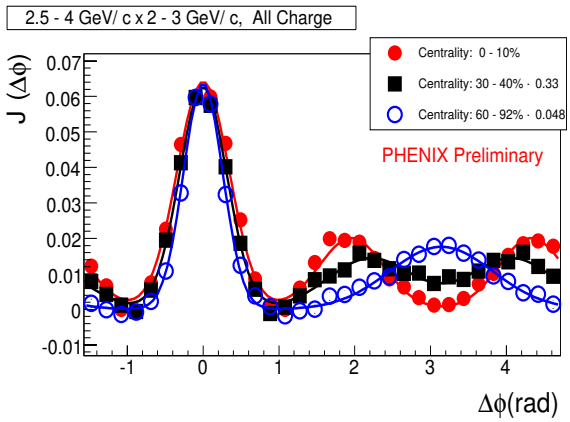

Figure 10. Correlation function for central, mid-central, and peripheral Au+Au collisions at $\sqrt{s_{NN}} = 200$ GeV after subtraction of the flow contribution [33].

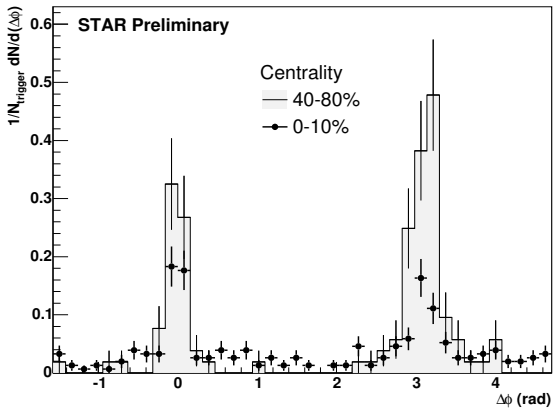

Figure 11. Azimuthal correlations of trigger photons ($E_T^{\rm trig} > 10$ GeV) with associated particles (4 GeV/c $< p_T^{\rm assoc} < E_T^{\rm trig}$) in central and peripheral Au+Au collisions [39].

increasing centrality, a feature that cannot be explained with the current jet quenching models. Exotic features like Cherenkov [35] or Mach cone [36] effects are being discussed in this context. Measurements of three-particle correlations will be very valuable to confirm the relevance of these new mechanisms. Active searches are underway and first results of three-particle correlations were shown at the conference [2,37].

The hadron-hadron correlations discussed so far are inherently limited by the trigger bias: the energy of the jet is not well defined by the trigger particle and the selected jets are preferentially created close to the surface. A much cleaner and unbiased picture can be obtained in prompt photon-hadron correlations in which the hadron trigger is replaced by a photon trigger. First attempts in this direction were presented at this conference [38,39]. An example is displayed in Fig. 11 showing azimuthal correlations of trigger photons ($E_T^{\rm trig} > 10$ GeV) with associated particles (4 GeV/c $< p_T^{\rm assoc} < E_T^{\rm trig}$) in central and peripheral Au+Au collisions [39].

6. Heavy Flavor

The heavy flavor results from RHIC are among the highlights of the conference. Contrary to expectations it was shown that heavy quarks flow and are strongly suppressed at high p_T. These results are inferred from measurements of non-photonic electrons which are assumed to originate from semi-leptonic decays mainly of c quarks at low p_T but with an increasing contribution of the heavier b quarks expected to dominate the electron yield at high enough p_T.

Fig. 12 shows the nuclear modification factor of non-photonic electrons measured by PHENIX [40] and STAR [13] in central Au+Au collisions. The two experiments are in good agreement here. Both show a very strong suppression with approximately the same shape and magnitude as for hadrons (see Figs. 5,6). This is a surprising result as the massive quarks are expected to radiate much less energy than the lighter u,d quarks. It forces the theoretical models which incorporate contributions both from charm and bottom quarks, to invoke a very high initial gluon density $dN_g/dy = 3500$ [42], a factor of ~ 3 higher than for π^0 (see Fig. 5), in order to reproduce the observed suppression.

It is a non-trivial challenge for the theorists to accommodate all the high p_T suppression results within a consistent theoretical framework. But there is also a not less demanding challenge for the experimentalists. The non-photonic electron results are derived from single electron measurements after subtracting large contributions from conversions and Dalitz decays. It is necessary to confirm and supplement these results with direct and separate measurements of the open charm and open bottom contributions. The first direct reconstruction of D mesons in Au+Au collisions reported by STAR is a first step in this direction [43] but it seems that more substantial progress will have to await for the implementation of the vertex detector upgrades which are currently under development both in PHENIX and STAR.

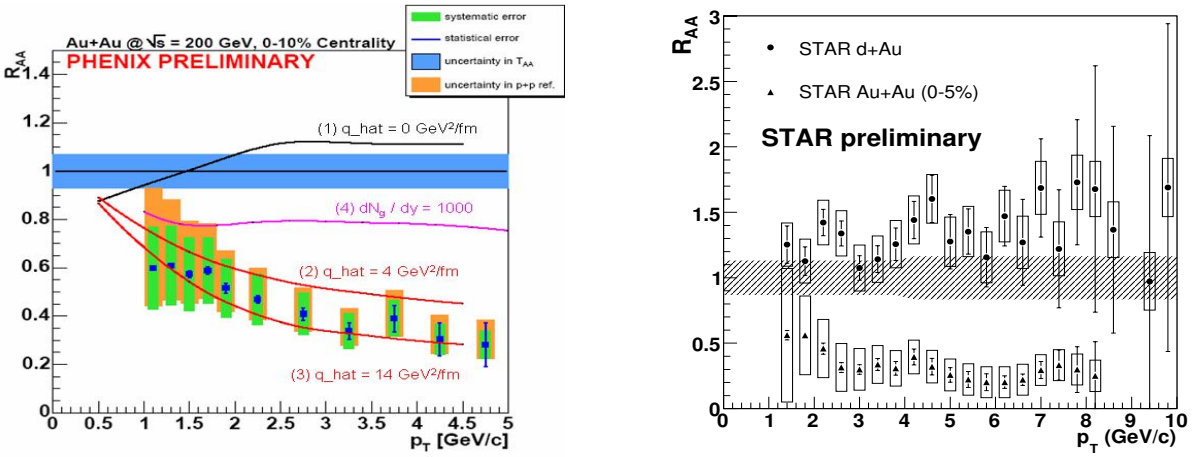

Figure 12. Nuclear modification factor of non-photonic electrons measured by PHENIX (left panel [40]) and STAR (right panel [13]) for central Au+Au collisions at $\sqrt{s_{NN}}$= 200 GeV. Theoretical predictions, curves (1)-(3) from [41] for charm quarks only and curve (4) from [42] for charm and bottom quarks, are shown on the left panel.

PHENIX reported measurements of elliptic flow v_2 of non-photonic electrons as function of p_T [40]. The results are shown in Fig. 13. The sizable flow observed at $p_T$values of 1-1.5 GeV/c, where the yield is dominated by semi-leptonic decays of open charm, indicates a sizable flow of D mesons. The flow seems to decrease to vanishing values at high p_T (the statistical errors are too large for a more conclusive statement) where the contribution from semi-leptonic bottom decays could be significant. A comparison to calculations with and without charm flow [44] favors the interpretation of charm flow. This implies a strong interaction with the medium and a high degree of thermalization of the charm quarks, again reinforcing the case for a strongly coupled QGP. Direct and separate measurements of D and B mesons elliptic flow will be very valuable to firmly and unambiguously establish the non-photonic electron results.

PHENIX has translated the non-photonic electron measurements in p+p and minimum bias Au+Au collisions at $\sqrt{s_{NN}}$ = 200 GeV into a total cross-section of charm production per nucleon-nucleon collision of $\sigma_{c\bar{c}}^{NN}$ = 0.92±0.15(stat.)±0.54(sys.) mb [45] and $\sigma_{c\bar{c}}^{NN}$ = 0.62±0.057(stat.)±0.16(sys.) mb [46], respectively. STAR has done a similar thing from the combined electron and direct D meson data in minimum bias d+Au ($\sigma_{c\bar{c}}^{NN}$ = 1.4±0.2(stat.)±0.2(sys.) mb) and Au+Au ($\sigma_{c\bar{c}}^{NN}$ = 1.11±0.08(stat.)±0.42(sys.) mb) measurements [43]. The PHENIX and STAR results are consistent within their large error

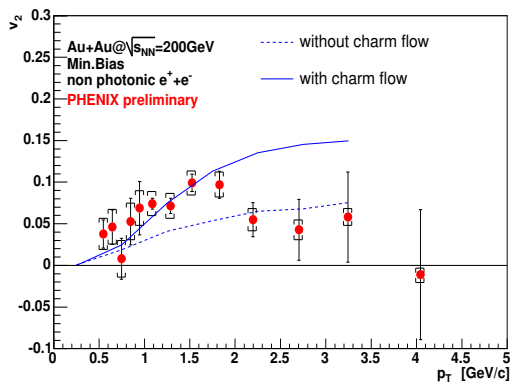

Figure 13. v_2 of non-photonic electrons, attributed to semi-leptonic open charm decays, measured by PHENIX [40] compared with theoretical predictions from [44].

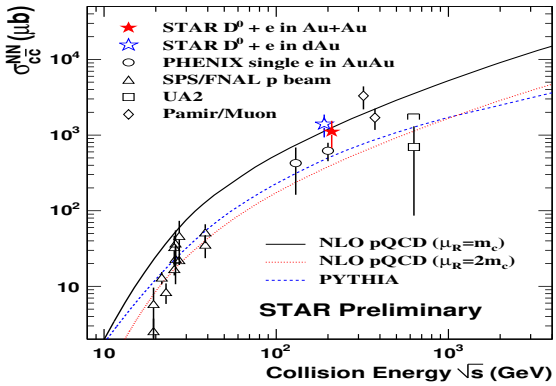

Figure 14. The $c\bar{c}$ cross section per binary collision vs. collision energy compared to NLO pQCD calculations[43].

bars and they support the scaling of the charm production cross section with the number of binary collisions. However, there is a factor of almost two difference in their minimum bias Au+Au cross sections. Larger precision is needed in view of the importance of this cross section in the evaluation of the J/ψ production through charm recombination (see Section 7) and to better constrain the NLO pQCD calculations. See Fig. 14 where the STAR and PHENIX results are plotted in a compilation of cross section vs. collision energy and compared to NLO pQCD calculations [43].

NA60 shed light on the long standing question of the origin of the dimuon excess at intermediate masses (m= 1.2 - 2.7 GeV/c^2) observed by NA50 in S+U and Pb+Pb collisions [47]. This excess can be interpreted as an enhancement of charm production in nuclear collisions as argued by NA50, or as evidence for thermal radiation [48,49]. NA60 confirmed that also in In+In collisions the dimuon yield at intermediate masses is enhanced over the expected contributions from Drell-Yan (fixed by the high mass region) and open charm (assuming $\sigma_{c\bar{c}}$=12 μb/nucleon), in very good agreement with the previous NA50 observations. But using displaced vertex information to tag the open charm semileptonic decays, NA60 was able to go one step further and to prove that the excess originates from a prompt source of dimuons rather than an enhanced open charm yield [50]. If it needed any proof, these results clearly illustrate the superiority of a direct measurement or tagging of D-mesons over more inclusive measurements.

7. J/ψ

The J/ψ production keeps generating great interest and remains an exciting topic. We have seen updated results from NA50, new results from NA60 and last but not least first results from PHENIX at RHIC. All these results taken together with the recent lattice calculations which predict the J/ψ to survive as a bound state in the QGP up to temperatures of $\sim 1.5 - 2T_c$, call for redefining the significance of the J/ψ production as *the* diagnostic tool of deconfinement at SPS and RHIC energies.

With a new determination of the J/ψ nuclear absorption cross section, derived from precision pA data, NA50 confirmed that the J/ψ yield in S+U and peripheral Pb+Pb col-

lisions is consistent with normal nuclear absorption. Only semi-central or central Pb+Pb collisions show an additional suppression (see Fig. 15) [51]. NA50 further characterized this anomalous suppression with two new results: (i)the suppression occurs mainly at low p_T. (ii) the central to peripheral ratios $R_{\rm CP}$ as function of p_T show an initial increase with p_T followed by a saturation at the level of 1 at higher p_T demonstrating binary scaling (see Fig. 12 of [51]).

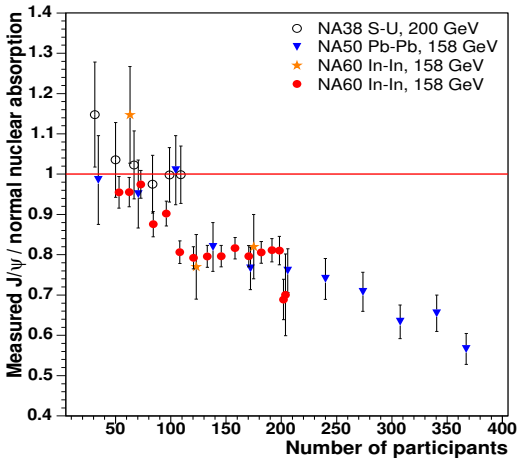

Figure 15. J/ψ suppression pattern measured in S+U, and Pb+Pb by NA50 and in In+In by NA60, as a function of N_{part} [50].

The first NA60 results on In+In collisions show also an anomalous J/ψ suppression. The pattern is very similar to the one observed by NA50 as illustrated in Fig. 15 where both results are overlayed together [50]. Within the accuracy of the measurements, the figure supports the claim already made in Section 3 that the number of participants seems to be a good scaling factor to take account of system size effects.

PHENIX presented results from a comprehensive set of J/ψ measurements. The set includes J/ψ production in p+p, d+Au, Cu+Cu and Au+Au collisions at $\sqrt{s_{NN}}$ =200 GeV and Cu+Cu at 62 GeV, at mid-rapidity ($|\eta| < 0.35$) through the e^+e^- decay channel and at forward rapidity ($|\eta| \in [1.2, 2.2]$) through the $\mu^+\mu^-$ decay channel [33]. The nuclear modification factor $R_{\rm AA}$ vs. centrality is shown in Fig. 16 for the $\sqrt{s_{NN}}$= 200 GeV data. There is a clear suppression and within the present errors, which are still too large, the PHENIX data show the same trend and the same magnitude of suppression irrespective of species and energy. Furthermore, the magnitude of the suppression, reaching a factor of ∼3 for the most central collisions, is similar to the one observed at the SPS.

This universality of the suppression is a surprising result. Models based on interactions with comovers [52], color screening [53], or QCD-inspired in-medium effects [54], which were able to explain the anomalous J/ψ suppression at the SPS, do predict a stronger suppression at the RHIC as one would intuitively expect due to the higher densities of RHIC (see left panel of Fig. 16).

The discrepancy is resolved by invoking the regeneration of J/ψ at a later stage of the collision via recombination of c and $\bar{c}$ quarks, more abundantly produced at RHIC. Several attempts in this direction [53–56], combining suppression and recombination, do reproduce

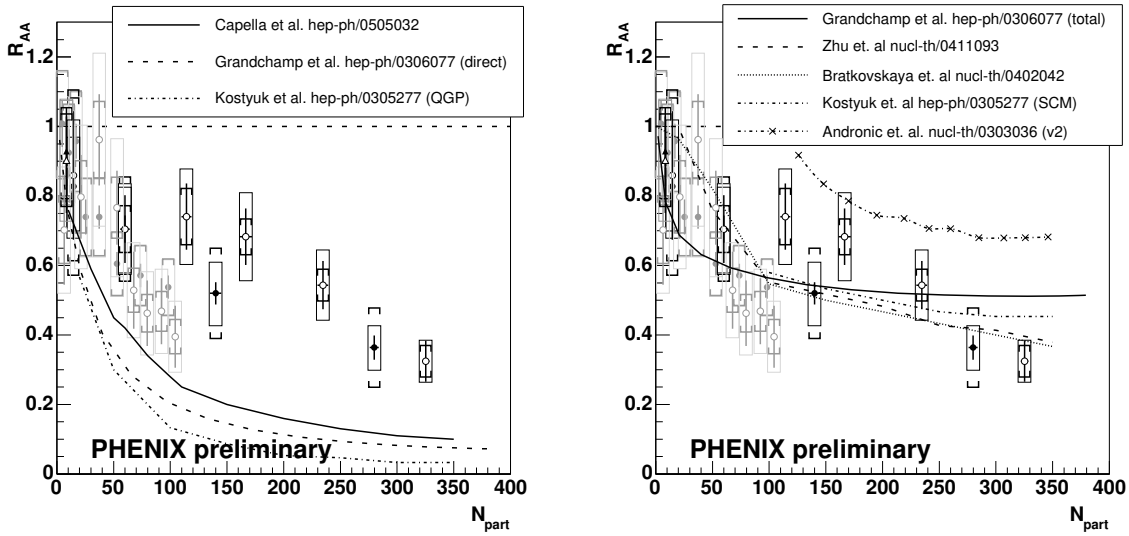

Figure 16. J/ψ nuclear modification factor as a function of the number of participants in d+Au, Au+Au and Cu+Cu measured by PHENIX at $\sqrt{s_{NN}} = 200$ GeV, compared to models which were able to explain the NA50 anomalous suppression (left panel) [52–54] and models involving either J/ψ regeneration by quark recombination [53–56] or J/ψ transport in medium [57] (right panel) [33].

the data reasonably well right panel of Fig. 16 [2]. This appears as an additional score in favor of the recombination models, whose success in explaining other aspects of the data, like e.g. the flow pattern at intermediate p_T was already emphasized. Recombination has however, additional consequences on J/ψ properties which should be corroborated by the data before it can be accepted as the dominant mechanism for J/ψ production at RHIC. First, the J/ψ rapidity distribution is expected to become narrower with increasing centrality, a feature not supported by existing results [58]. (This negative observation should be taken with some reservation since it is based on results suffering from large uncertainties). Second, the J/ψ should exhibit a high p_T suppression pattern compatible with the one observed for charm quarks (see Section 6). Finally the J/ψ should exhibit elliptic flow consistent with the flow observed for charm quarks. Results on this crucial test are not yet available. For a better scrutiny of the recombination models we thus need more precise data on the rapidity distribution and high p_T suppression of the J/ψ and equally precise data on elliptic flow. A more accurate determination of the charm production cross section is also essential. On the theory side, firm predictions of the correlations between the properties of c quarks and J/ψ are also needed.

Another interesting possibility, appealing for its simplicity, has been proposed that could explain all the SPS and RHIC results. The anomalous J/ψ suppression would originate from the total melting of excited charmonium states, in particular the χ_c, that feed the J/ψ and account for about 40% of its yield [59]. This is supported by recent lattice QCD calculations according to which, at the temperatures reached at SPS and RHIC energies, only the ψ' and χ_c are dissolved by color screening in the QGP, whereas the J/ψ remains as a bound state up to temperatures of $\sim 1.5 - 2T_c$ [60,61]. If this explanation holds true, we will have to wait to the LHC, where the temperature will be high enough, to observe

[2] the figure includes also calculations based on J/ψ transport in the QGP [57] which are also in reasonable agreement with the data.

the suppression of directly produced J/ψ.

8. Low-mass dileptons

Many new and significant results have been presented at this conference: first attempts of PHENIX to measure low-mass electron pairs from the 2004 high luminosity Au+Au run, almost final results of CERES from the 2000 Pb+Au run and last but not least, the superb data of NA60 on In+In collisions.

PHENIX has an excellent mass resolution (approximately 1% at the ϕ meson mass) and good electron identification capabilities in the central arms, based on a RICH detector and an electro-magnetic calorimeter. However, the limited azimuthal acceptance in the central arms and the strong magnetic radial field beginning at the vertex, make the identification and rejection of the relatively large number of electron-positron pairs from Dalitz decays and photon conversions very difficult, resulting in an overwhelming combinatorial background. In the present set-up the signal to background S/B ratio for masses m = 0.2 - 0.5 GeV/c^2 is smaller than 1/100 as illustrated in the left panel of Fig. 17 [62]. PHENIX has mastered the background subtraction technique to a very high level of preci-

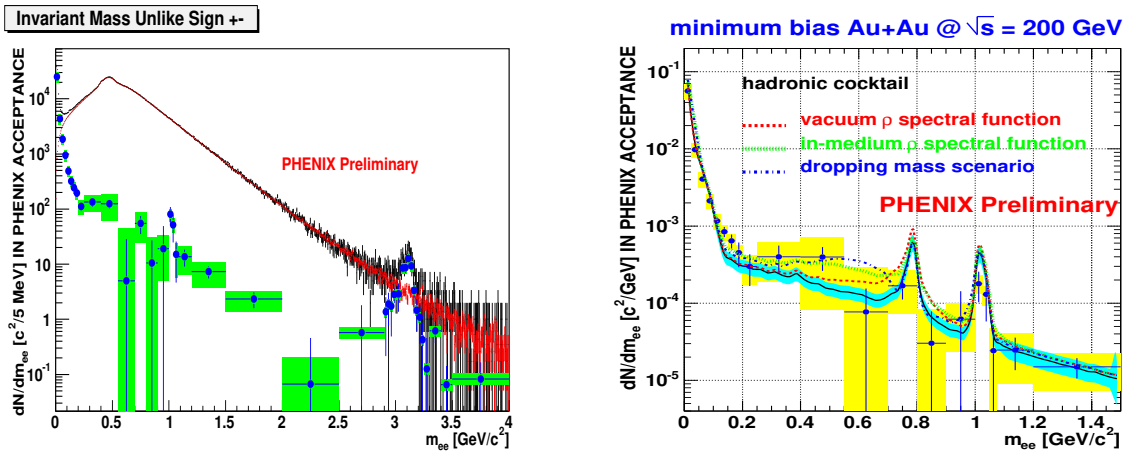

Figure 17. Low-mass dilepton results of PHENIX in Au+Au collisions at $\sqrt{s_{NN}}$ = 200 GeV. Left panel: measured unlike sign (black), mixed events background (red), and subtracted (blue), mass spectra. Right panel: subtracted mass spectrum compared to model predictions [65] and to a pure hadronic cocktail [62]

sion (±0.25%). But with a S/B < 1/100 this is not sufficient. The statistical significance of the measurement is largely reduced and the systematic uncertainty is large preventing any conclusive interpretation of the data. The right panel of Fig. 17 shows the background subtracted spectrum compared to a pure cocktail of expected sources (hadronic decays and semi-leptonic open charm decay) as well as several model predictions [65] including the vacuum ρ spectral function, the in-medium ρ broadening and the in-medium ρ dropping mass. Differences as large as a factor of three between the various predictions cannot be resolved within the present uncertainties of the data. PHENIX has also the potential of measuring the ϕ meson through the e^+e^- and K^+K^- decay channels. Although the S/B ratio in the $\phi \to e^+e^-$ is somewhat better (S/B $\sim$ 1/60) the errors are still too large for a meaningful comparison to the much higher precision of the $\phi \to K^+K^-$ data [66]. Larger

data samples will be of very limited help. A breakthrough in the PHENIX capabilities to measure low-mass dileptons is expected with the installation foreseen in 2006, of the Hadron Blind Detector [63] presently under construction [64].

CERES presented almost final results of the 2000 Pb+Au run with the upgraded spectrometer with a radial TPC. The absolutely normalized invariant mass spectrum of electron pairs shows a clear excess with respect to the hadron cocktail of expected sources, at masses m $>$ 0.2 GeV/c^2 (see Fig. 4 in ref. [67]). The magnitude of the excess and its p_T dependence are in very good agreement with previous CERES results. With the improved mass resolution a hint of the ω and ϕ meson peaks is seen for the first time in the CERES data. The results are compared in Fig. 18 to calculations performed by Rapp [68] including in-medium modifications of the ρ meson (dropping mass according to the Brown-Rho scaling [69], broadening of the ρ according to the Rapp-Wambach model [70]). The figure also shows a calculation by Kaempfer based on a parametrization of the dilepton yield in terms of $q\bar{q}$ annihilation inspired by quark-hadron duality [71]. Whereas the three calculations give very similar results for masses m $<$ 0.8 GeV/c^2 where the precision of the data is insufficient to discriminate between them, it is interesting to note that the pronounced minimum between the ω and the ϕ in the dropping mass scenario, as implemented in the Rapp calculations, is not seen in the data.

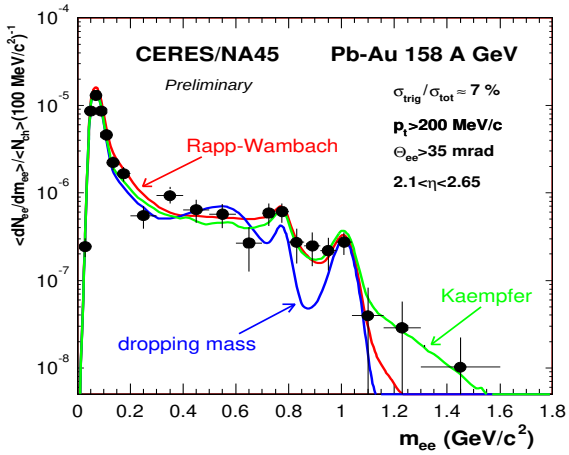

Figure 18. Dielectron mass spectrum measured by CERES compared to calculations performed by Rapp (curves labeled Rapp-Wambach and dropping mass) [68] and by Kaempfer [71] (see text for further details) [67].

The highlight on low-mass dileptons belongs without any doubt to NA60. With an excellent mass resolution of 2.2% at the ϕ mass and excellent statistics, NA60 presented high quality results on low-mass dimuons in 158 AGeV In+In collisions [50,72]. The data show a clear excess of dimuons which increases with centrality and is more pronounced at low pair p_T. The results confirm, and are consistent (at least qualitatively) with, the pioneering CERES results over the last ten years. NA60 also showed (see Fig. 19) the excess mass spectrum, obtained after subtracting from the data the hadronic cocktail without the ρ (see [72] for details of the subtraction procedure). The excess exhibits a broad structure, with a width increasing with centrality, centered at the nominal position of the ρ meson mass. The figure shows also a comparison of the excess with model calcula-

tions [73] including the vacuum ρ (thick dashed line), in-medium ρ broadening (thick solid line) according to the Rapp-Wambach model [70] and dropping ρ mass (dashed-dotted line). The comparison clearly favors the in-medium broadening of the ρ meson over the dropping mass scenario as implemented in [73]. The conclusions are valid also for other centralities and as function of p_T.

The NA60 data certainly pose a new constraint on the theoretical models which will have to simultaneously account for the CERES and NA60 results. But the deeper impact of these results is their possible relevance to the broader context of chiral symmetry restoration. If the system reaches, or is near to, chiral symmetry restoration then the dilepton results could be telling us that the approach to such a state proceeds through broadening and eventually subsequent melting of the resonances rather than by dropping masses or mass degeneracy between chiral partners.

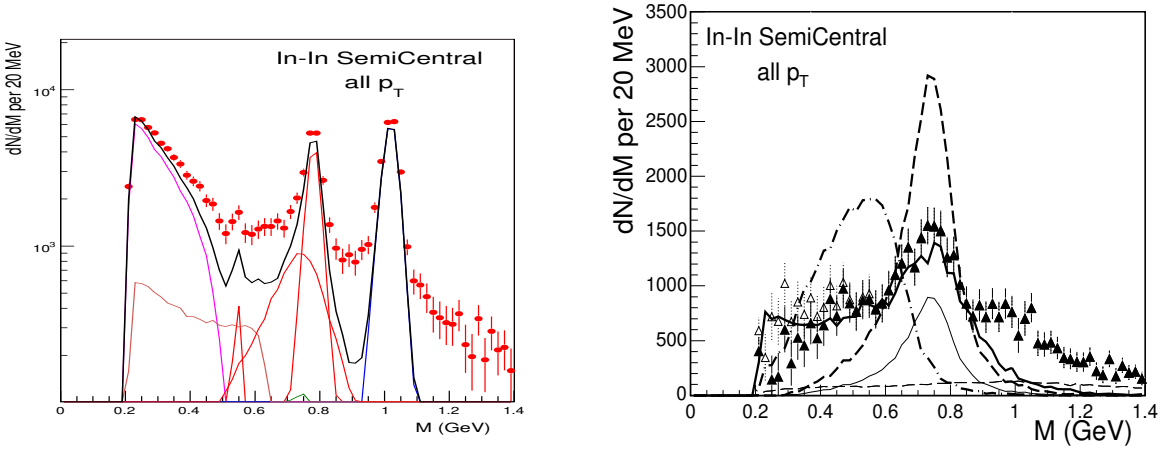

Figure 19. NA60 dimuon results in semi-central In+In collisions. Left panel: mass spectrum compared to hadronic cocktail. Right panel: excess mass spectrum compared to the cocktail ρ (thin solid line), open charm decays (thin dashed line), and calculations [73] including the vacuum shape (thick dashed line), in-medium broadening (thick solid line) and dropping mass (dashed dotted line), of the ρ [72].

9. Photons

Using a novel analysis technique based on low-mass electron pairs with high p_T, PHENIX presented interesting and intriguing results on direct photons. Exploiting the fact that any source of real γ photons emits also virtual γ^* photons with very low-mass, the low-mass electron pair yield (after taking into account the contribution from Dalitz decays) is translated into a direct photon spectrum assuming $\gamma_{direct}/\gamma_{incl.} = \gamma^*_{direct}/\gamma^*_{incl.}$ [74,75]. The resulting direct photon spectrum is shown in Fig. 20. It is compatible with the spectrum obtained from a conventional analysis of inclusive real photons [76] but it has smaller error bars giving more significance to the signal and allowing to extend its range down to p_T= 1 GeV/c. These two improvements are crucial in making apparent an excess of direct photons in the p_T range of 1 to 4 GeV/c, over NLO pQCD calculations [78], which is then ascribed to emission from the medium. Interpreted as the elusive thermal radiation of the QGP, the excess spectrum implies an initial temperature of 570 MeV or an average temperature of 360 MeV [77], in the plasma. But is this a unique interpretation? Are these

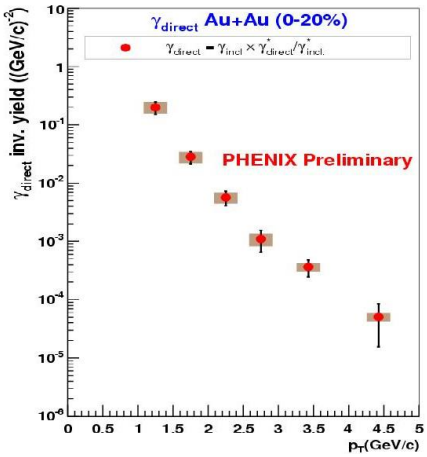

Figure 20. p_T distribution of direct photons measured by PHENIX in central Au+Au collisions at $\sqrt{s_{NN}} = 200$ GeV [75].

direct photons of thermal origin? More studies, in particular applying the same analysis technique to reference measurements of p+p and d+Au, are needed to consolidate the findings.

10. Outlook

To summarize the summary, this was a great conference. I tried to focus here on the highlights among the many new and exciting results that were presented. In the "Focus" talks, STAR summarized its results [79] and PHENIX synthesized its findings [75] drawing the emerging picture that characterizes the matter formed at RHIC. A very high density, strongly interacting partonic matter (made of constituent quarks) is formed, reaching thermal equilibrium very early in the collision and behaving like a perfect fluid with a very low (zero?) viscosity. This is not the ideal QGP gas of free quarks and gluons that we have been looking for during almost twenty years. This discovery is still ahead of us. The higher energies of the LHC might be needed for that. As emphasized in the Introduction, RHIC has accomplished a lot but much is left to do. We are only starting to examine the detailed properties of the matter formed at RHIC using the full panoply of penetrating probes: jets, open and hidden charm, low-mass dileptons and photons . Many questions are still open, e.g. we have not yet seen unambiguous evidence for deconfinement or chiral symmetry restoration. These questions are high on the RHIC agenda and will be addressed in the next few runs. With the RHIC upgrades coming online and the LHC glimpsing over the horizon, I look forward to sustained progress and more exciting results over many years.

11. Acknowledgements

This work was supported by the Israel Science Foundation, the US-Israel Binational Science Foundation, the MINERVA Foundation and the Leon and Nella Benoziyo Center for High Energy Physics. I am grateful to David D'Enterria, Zeev Fraenkel, Peter Jacobs, Roy Lacey and Xin-Nian Wang for useful comments and discussions. Finally I wish to thank the QM05 organizers and in particular Péter Lévai and Tamás Csörgő for such a wonderful and fruitful conference.

REFERENCES

1. The four white-papers were published in a special volume, Nucl. Phys. **A757**, 2005.
2. F. Wang, for the STAR Coll., nucl-ex/0510068 and these proceedings.
3. V. Greene, for the PHENIX Coll., these proceedings.
4. M. Oldenburg, for the STAR Coll., nucl-ex/0510026 and these proceedings.
5. R.A. Lacey, nucl-ex/0510029 and these proceedings.
6. R.J. Fries, B. Muller, C. Nonaka and S.A. Bass, Phys. Rev. Lett. 90 (2003) 202303 and Phys. Rev. C68 (2003) 044902.
7. D. Molnar and S.A. Voloshin, Phys. Rev. Lett. 91 (2003) 092301.
8. D. Winter, for the PHENIX Coll., nucl-ex/0511039 and these proceedings.
9. J. Adams *et al.*, Phys. Rev. Lett. 93 (2004) 252301.
10. G. Stefanek, for the NA49 Coll., nucl-ex/0510067 and these proceedings.
11. J. Milosevic, for the CERES Coll., nucl-ex/0510057 and these proceedings.
12. G. Roland, for the PHOBOS Coll., nucl-ex/0510042 and these proceedings.
13. J. Dunlop, for the STAR Coll., nucl-ex/0510073 and these proceedings.
14. P. Staszel, for the BRAHMS Coll., nucl-ex/0510061 and these proceedings.
15. H. Masui, for the PHENIX Coll., nucl-ex/0510018 and these proceedings.
16. P. Jacobs and M. van Leeuwen, nucl-ex/0511013 and these proceedings.
17. B. Cole, these proceedings.
18. M. Shimomura, for the PHENIX Coll., nucl-ex/0510023 and these proceedings.
19. I. Vitev and M. Gyulassy, Phys. Rev. Lett. 89 (2002) 252301.
20. X.N. Wang, Phys. Lett. B595 (2004) 165.
21. K. Eskola *et al.*, Nucl. Phys. A747 (2005) 511.
22. O. Barannikova, for the STAR Coll., these proceedings.
23. R.C. Hwa and C.B. Yang, Phys. Rev. C70 (2003) 024904.
24. V. Greko, C.M. Ko and P. Levai, Phys. Rev. C68 (2003) 034904.
25. A. Laszlo and T. Schuster, for the NA49 Coll., nucl-ex/0510054 and these proceedings.
26. A. Dainese, for the NA57 Coll., nucl-ex/0510082 and these proceedings.
27. S. Salur, for the STAR Coll., nucl-ex/0509036 and these proceedings.
28. E. Shuryak, Phys. Rev. C66 (2002) 027902.
29. X.N. Wang, private communication.
30. J. Adler *et al.*, Phys. Rev. Lett. 90 (2003) 082302.
31. J. Adams *et al.*, Phys. Rev. Lett. 95 (2005) 152301.
32. D. Magestro, for the STAR Coll., nucl-ex/0509030 and these proceedings.
33. H. Buesching, for the PHENIX Coll., nucl-ex/0511044 and these proceedings.
34. A. Majumder, E. Wang and X.N. Wang, nucl-th/0412061.
35. A. Majumder and X.N. Wang, nucl-th/0507062.
36. J. Casalderrey-Solana, E.V. Shuryak and D. Teaney, hep-ph/0411315.
37. N.N. Ajitanand, for the PHENIX Coll., nucl-ex/0510040 and these proceedings.
38. N. Grau, for the PHENIX Coll., nucl-ex/0511046 and these proceedings.
39. T. Dietel, for the STAR Coll., nucl-ex/0510046 and these proceedings.
40. S. Butsyk, for the PHENIX Coll., nucl-ex/0510010 and these proceedings.
41. N. Armesto, S. Dainese, C. Salgado and U. Wiedemann, Phys. Rev. D71 (2005) 054027.

42. M. Djordjevic, M. Gyulassy, R. Vogt and S. Wicks, nucl-th/0507019, Phys. Lett. B in press.
43. H. Zhang, for the STAR Coll., nucl-ex/0510033 and these proceedings.
44. V. Greco, C.M. Ko and R. Rapp, Phys. Lett. B595 (2004) 202.
45. S.S. Adler *et al.*, Phys. Rev. Lett. in press, hep-ex/0508034.
46. S.S. Adler *et al.*, Phys. Rev. Lett. 94 (2005) 082301.
47. M.C. Abreu, Eur. Phys. J. C14, (2000) 443.
48. R. Rapp and E.V. Shuryak, Phys. Lett. B473 (2000)13.
49. G.Q. Li and C. Gale, Phys. Rev. Lett. 81 (1998) 1572.
50. E. Scomparin, for the NA60 Coll., these proceedings.
51. L. Ramello, for the NA50 Coll., these proceedings.
52. A. Capella and E.G. Ferreiro, Eur. Phys. J. C42 (2005) 419.
53. A.P. Kostyuk, M.I. Gorenstein, H. Stoecker and W. Greiner, Phys. Rev. C68 (2003) 041902.
54. L. Grandchamp, R. Rapp and G.E. Brown, Phys. Rev. Lett. 92 (2004) 212301.
55. E.L. Bratkovskaya, A.P. Kostyuk, W. Cassing and H. Stoecker, Phys. Rev. C69 (2004) 054903.
56. A. Andronic, P. Braun-Munzinger, K. Redlich and J. Stachel, Phys. Lett. B571 (2003) 36.
57. X.L. Zhu,P.F. Zhuang and N. Xu, Phys. Lett. B607 (2005)107.
58. H. Pereira Da Costa, for the PHENIX Coll., nucl-ex/0510051 and these proceedings.
59. M. Nardi, these proceedings.
60. M. Asakawa and T. Hatsuda, Phys. Rev. Lett. 92 (2004) 012001.
61. S. Datta, F. Karsch, P. Petreczkyand I. Wetzorke, Phys. Rev. D69 (2004) 094507.
62. A. Toia, for the PHENIX Coll., nucl-ex/0510006 and these proceedings.
63. A. Kozlov *et al.*,Nucl. Instr. and Meth. A523 (2004) 345 and Z. Fraenkel *et al.*, Nucl. Instr. and Meth. A546 (2005)466.
64. I. Ravinovich, for the PHENIX Coll., nucl-ex/0510024 and these proceedings.
65. R. Rapp, Phys. Rev. C63 (2001) 054907 and nucl-th/0204003.
66. A. Kozlov, for the PHENIX Coll., nucl-ex/0510016 and these proceedings.
67. D. Miskowiec, for the CERES Coll., nucl-ex/0511010 and these proceedings.
68. R. Rapp, private communication to the CERES Coll..
69. G.E. Brown and M. Rho, Phys. Rev. Lett. 66 (1991) 2720 and Phys. Rep. 269 (1996) 333.
70. R. Rapp and J. Wambach, Adv. Nucl. Phys. 25 (2000) 1.
71. K. Gallmeister, B. Kaempfer, O.P. Pavlenko and C. Gale, Nucl. Phys. A688 (2001) 939.
72. S. Damjanovic, for the NA60 Coll., nucl-ex/0510044 and these proceedings.
73. R. Rapp, private communication to the NA60 Coll..
74. S. Bathe, for the PHENIX Coll., nucl-ex/0511041 and these proceedings.
75. Y. Akiba, for the PHENIX Coll., nucl-ex/0510008 and these proceedings.
76. S.S. Adler *et al.* PHENIX Coll., Phys. Rev. Lett. 94 (2005) 232301.
77. D. d'Enterria and D. Peressounko, nucl-th/0503054.
78. L.E. Gordon and W. Vogelsang, Phys. Rev. D48 (1993) 3136.
79. C. Gagliardi, for the STAR Coll., nucl-ex/0512043 and these proceedings.